Bubbles—a glass-ceramic plague

By Oscar Peitl and Edgar D. Zanotto

Understanding the mechanism behind bubble formation in glass-ceramics can lead to the creation of bubble-free glass. An experimental "bubble map" could help increase understanding.

Glass-ceramics (GC) were discovered by S. D. Stookey approximately 65 years ago.[1] GC research and technology can now be considered a mature field described by over 10,000 scientific articles and 5,000 patents, although many other GC may still be discovered, and a plethora of issues pertaining to their development and production remain to be solved.[1–4]

Deubener et al.[5] (2018) recently described GCs thus: "Glass-ceramics are inorganic, non-metallic materials prepared by controlled crystallization of glasses via different processing methods. They contain at least one type of functional crystalline phase and a residual glass. The volume fraction crystallized may vary from ppm to almost 100%." GCs can be produced by sintering with concurrent surface crystallization of crushed glass powders or more traditionally by catalyzed internal crystallization of monolithic glass articles.[1–5]

Sintered GCs usually contain some residual porosity that degrades most of their properties, especially optical transparency and fracture strength.[6–10] However, in some situations—such as the development of insulation materials, substrates for catalytic converters, or bioactive scaffolds—pores are desirable and therefore deliberately induced. This short article does not discuss residual pores in sintered GCs because that topic has been examined and reported in several studies.[6–10]

One facet that is likely familiar to industrial GC researchers but is not well known by the glass research community is that even traditional GCs are frequently plagued with bubbles, which appear after partial crystallization of bubble-free glasses. However, to the best of our knowledge (and surprisingly), the microstructural conditions that favor spontaneous bubble formation in traditional GCs have been mostly overlooked and underreported.

Our interest in this research work focused on understanding the causes of (undesirable) porosity that sometimes forms during glass crystallization. There are two main mechanisms of pore or bubble

Capsule summary

BUBBLES ARE A BOTHER

Glass-ceramics are frequently plagued with bubbles, which appear after partial crystallization of bubble-free glasses. However, the microstructural conditions that favor spontaneous bubble formation have been mostly overlooked and underreported.

STOPPING BUBBLE FORMATION

A "bubble map," an experimental diagram showing regions of bubble formation as a function of crystallinity and crystal size, can be a useful tool for developing bubble-free glass-ceramics.

THE ROLE OF GAS

A bubble map for 1.07N2C3S showed bubbles tend to grow in glass-ceramics containing high crystallinity and large crystal sizes, suggesting that crystals can absorb less dissolved gases than the liquid phase.

nucleation and growth in (nonsintered) traditional GCs: i) large density misfits between parent glass and crystal phases,[11] and ii) the release of dissolved gases during crystallization, which become supersaturated when the crystallized volume fraction increases.[12-13] In this paper, we compile and discuss experimental results involving the second mechanism.

We believe that current knowledge about spontaneous pore formation in traditional GCs may be disguised as an industrial secret. To a large extent, academic researchers have ignored this bubble formation mechanism, typically limiting themselves to statements such as "the glass-ceramic microstructure consists of ... crystal phases, a residual glass, and some porosity...," without seeking to determine the conditions for and causes of such porosity.

In this work, we carried out an experimental study of bubble formation in a specially designed soda-lime-silica GC, by systematically varying its microstructure in terms of crystallized volume fraction and crystal size. Using this GC as an example, we constructed, for the first time, an experimental "bubble map," i.e., a pore-free zone in a crystallized fraction versus average crystal size plot. In a subsequent study, we intend to discuss in detail the cause of bubble formation in this particular GC, and will also present similar results obtained for other types of GCs that show crystallization-induced bubbles.

Material and methods

The desired $1.07Na_2O.2CaO.3SiO_2$ glass (1.07N2C3S) that shows copious internal nucleation was produced using Na_2CO_3 (99.8 percent) and $CaCO_3$ (99.9 percent), both from Merck, USA, and quartz sand (99.99 percent) from Vitrovita, Brazil. Proper amounts of these chemicals were weighed and mixed in a powerful planetary mixer for two hours. They were then placed in a platinum crucible and melted for two hours between 1,300–1,360°C in an electric furnace, poured three times, crushed and remelted, and finally cast into a cylindrical graphite mold 8 mm in diameter and 35 mm in length. The glass samples were then subjected to an annealing treatment at 550°C (T_g ~ 570°C), held there for three hours, and slowly cooled. Finally, using a diamond disk cutter operating at low speed, disk-shaped specimens were cut into approximately 3 mm thick slices and chemically analyzed by X-ray fluorescence, which confirmed the actual composition was close to the target one.

A two-stage heat treatment was employed to determine the crystal nucleation kinetics at various temperatures. The number of crystals per unit area were determined by optical microscopy and analyzed as a function of the nucleation time at different temperatures. After counting approximately 300 crystals per heat treatment, the number of crystals per unit area (N_S) was determined using reflected light optical microscopy. The average number of crystals per unit volume (N_V) was then calculated using a standard stereological formula. Crystal growth rates were determined by the same method as that used to estimate the nucleation rates. After heat treatment at a given nucleation temperature (T_N) for time t_n—which was designed to produce only a small amount of crystal-

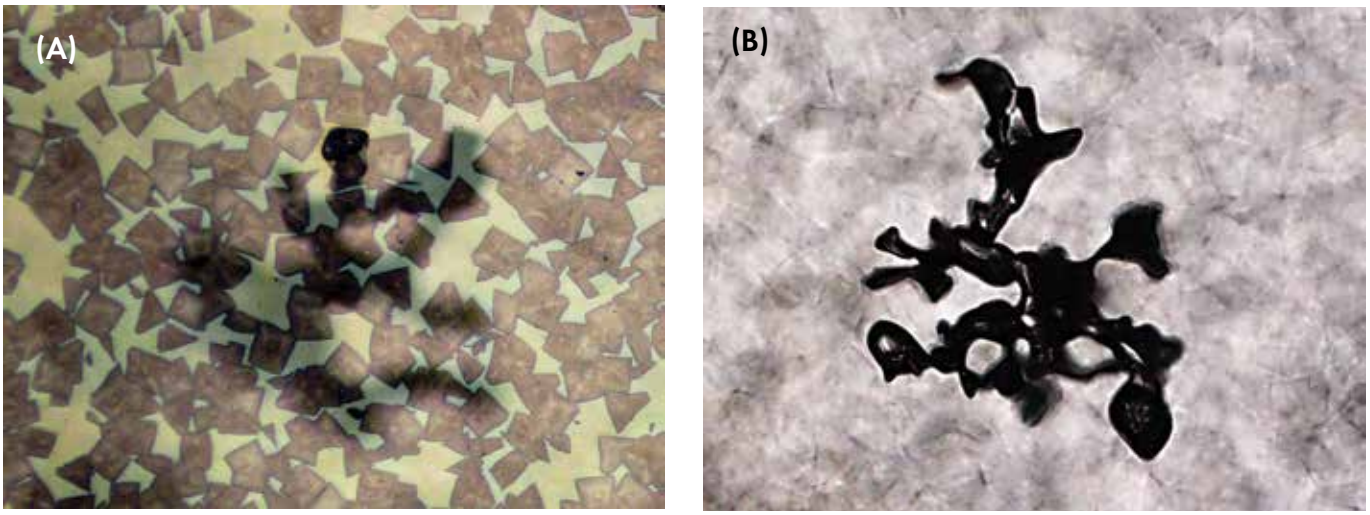

Credit: Zanotto

Figure 1. Optical micrographs of the 1.07N2C3S glass-ceramic, showing crystals and bubbles by reflected light (A); and transmitted light mode (B) highlighting the bubble structure. Micrograph A was taken from a surface polished with cerium oxide (1 μm) after etching with a diluted solution of HF (0.1 percent) + HCl (0.05 percent). The largest crystal size is approximately 50 microns.

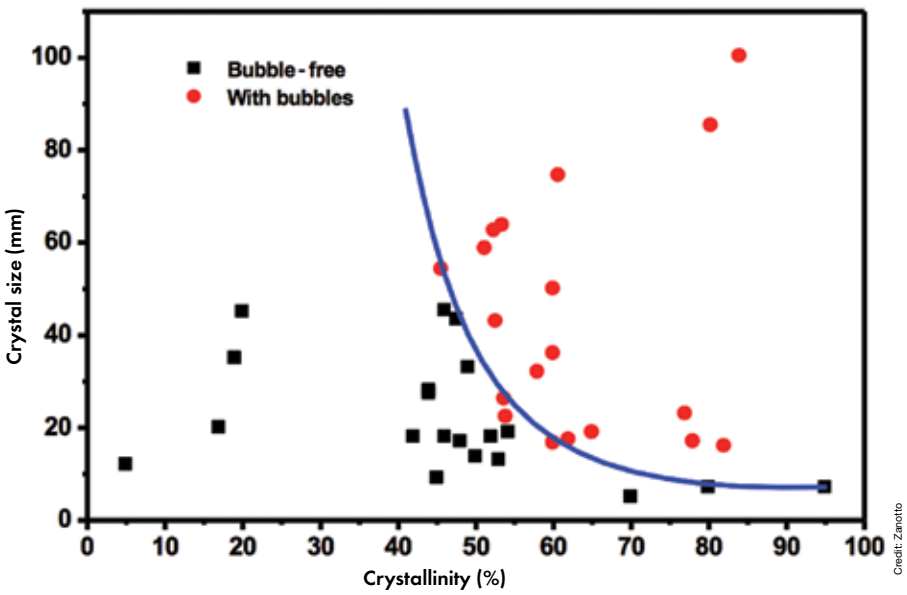

Figure 2. Bubble map of the 1.07N2C3S glass-ceramic. The red spheres indicate the region undergoing bubble formation, whereas the black squares show the bubble-free microstructural conditions.

line nuclei—the samples were "developed" at a temperature T_C for various times t_c. The growth rates were then determined from the slope of crystal size versus time plots at 675°C and 700°C. These estimated nucleation and growth curves were used to design several microstructures employed to create a pore map.

Results and discussion

Figure 1 shows examples of a bubble inside a partially crystallized GC. These micrographs were recorded using a Nikon Eclipse LV100N POL optical microscope. Two methods were applied to the same region of the sample and same magnification: Figure 1A, using reflected light; and Figure 1B, using transmitted light. Figure 1A shows a cross-section with quasi-cubic crystals, the residual glass matrix, three pores, and a shadow surrounding them. These bubbles are immersed in the residual glass phase, and hence were probably formed at the crystal/liquid interfaces and grew into the liquid phase during crystallization. The shadows are due to the interconnected shape of the bubbles, which are not individually separated spheres, as commonly observed in ordinary glasses. Micrograph 1B, which highlights the complex 3D bubble structure snaking across the crystals, was recorded using an accessory that allows one to obtain images by step scanning the *z*-axis and assemble them using dedicated software.

It should be noted that these bubbles are located not at the surface of the sample but inside the glass. The nucleation rate at glass surfaces is greatly enhanced by defects, dust, cracks, and flaws.[14–15] Hence, glass surfaces usually crystallize completely during crystal growth treatments, while the crystallized volume fraction at the center of the sample remains relatively low. A degassing effect begins (to be further described in this article) as crystallization proceeds.

The "bubble map" in Figure 2 shows the microstructural conditions that favor bubble/pore formation (black squares) in a crystal size versus volume fraction crystallized plot for the 1.07N2C3S glass-ceramic.

This diagram indicates that a large transformed volume fraction (in this case, greater than 50 percent) leads to pore formation, suggesting that some dissolved gas becomes supersaturated in the liquid phase and is expelled at the crystal growth front. However, in three experiments with crystallized volume fractions of up to 95 percent, no bubbles were formed when the average crystal size was smaller than 10 μm.

To generalize (or not) the current findings, we conducted the same type of experiment with a stoichiometric lithium disilicate ($Li_2O.2SiO_2$) glass and confirmed that a similar bubble map profile could be created. The results will be demonstrated and discussed in detail in a forthcoming paper.

To identify the type of gas inside the bubbles, a series of GC samples containing visible bubbles were prepared. The samples were then broken up under vacuum at room temperature, using a screw that presses the sample against a wall and produces a partial fracture. At each turn of the screw another portion of the sample was fractured, releasing gases that were trapped in the pores. These gases were analyzed by an inductively coupled plasma mass spectrometer. The results confirmed the presence of (at least) oxygen. More in-depth studies are needed to understand the formation of oxygen and to check for the presence of other gases.

We then hypothesize that, since most crystals can absorb less dissolved gases than the liquid phase, an increase in the microstructure's crystallinity likely leads to gas supersaturation in the liquid, favoring bubble nucleation at the crystal/liquid interface. Therefore, it is understandable that bubbles are formed at the crystal/glass interface and grow into the liquid phase. However, it is still not clear why, even with very high transformed volume fractions, relatively small crystals do not trigger bubble formation. This finding warrants further study.

Conclusions

We proposed and created, for the first time, a bubble map—an experimental diagram showing bubble formation as a function of the percentage of crystallinity and average crystal size—for a $1.07Na_2O.2CaO.3SiO_2$ glass-ceramic. The diagram demonstrates that bubbles tend to nucleate and grow in GCs containing high crystallized volume fractions and large crystal sizes. A rational explanation is therefore that crystals can absorb less dissolved gases than the liquid phase. Hence, increased crystallinity leads to gas supersaturation in the liquid, favoring bubble nucleation at the crystal/liquid interface.

Further studies are necessary to pinpoint the cause of bubble formation in other GCs. Be that as it may, the creation of bubble maps can be a useful strategy for the development of bubble-free GCs.

Acknowledgements

The authors are indebted to the São Paulo Research Foundation, FAPESP, Brazil, for its generous funding through the CEPID Program (Process # 2013/007796-3). We are grateful to George Beall for his valuable suggestions.

About the authors

Oscar Peitl is adjunct professor and Edgar D. Zanotto is professor of materials science and engineering in the Center for Research, Technology, and Education in Vitreous Materials at the Federal University of São Carlos. Contact Zanotto at dedz@ufscar.br.

References

[1]Holand, W. & Beall, G.H. (2012). *Glass Ceramic Technology: Second Edition*. Hoboken, NJ: John Wiley & Sons.

[2]Davis, M.J. & Zanotto, E.D. (2017). Glass-ceramics and realization of the unobtainable: Property combinations that push the envelope. *MRS Bulletin*, **42**(3), pp. 195–199.

[3]Montazerian, M., Singh, S.P., & Zanotto, E.D. (20150. An analysis of glass-ceramic research and commercialization. *American Ceramic Society Bulletin*, **94**(4), pp. 30–35.

[4]Zanotto, E.D. (2010). A bright future for glass-ceramics. *American Ceramic Society Bulletin*, **89**(8), pp. 19–27.

[5]Deubener, J., Allix, M., Davis, M.J., Duran, A., Höche, T., ... & Zhou, S. (2018). Updated definition of glass-ceramics. *Journal of Non-Crystalline Solids*, **501**, pp. 3–10.

[6]Karamanov, A. & Pelino, M. (2008). Induced crystallization porosity and properties of sintered diopside and wollastonite glass-ceramics. *Journal of the European Ceramic Society*, **28**(3), pp. 555–562.

[7]Karamanov, A. & Pelino, M. (2006). Sinter-crystallisation in the diopside-albite system. Part I. Formation of induced crystallisation porosity. *Journal of the European Ceramic Society*, **26**(13), pp. 2511–2517.

[8]Prado, M.O., Fredericci, C., & Zanotto, E.D. (2003). Isothermal sintering with concurrent crystallization of polydispersed soda-lime-silica glass beads. *Journal of Non-Crystalline Solids*, **331**(1–3), pp. 145–156.

[9]Prado, M.O., Fredericci, C., & Zanotto, E.D. (2003). Non-isothermal sintering with concurrent crystallization of polydispersed soda-lime-silica glass beads. *Journal of Non-Crystalline Solids*, **331**(1–3), pp. 157–167.

[10]Prado, M.O. & Zanotto, E.D. (2002). Glass sintering with concurrent crystallization. *Comptes rendus Chimie*, **5**(11), pp. 773–786.

[11]Fokin, V.M., Abyzov, A.S., Schmelzer, J.W.P., & Zanotto, E.D. (2010). Stress induced pore formation and phase selection in a crystallizing stretched glass. *Journal of Non-Crystalline Solids*, **356**(33–34), pp. 1679–1688.

[12]Heide, K., Hartmann, E., Stelzner, Th., & Müller, R. (1996). Degassing of a cordierite glass melt during nucleation and crystallization. *Thermochimica Acta*, **280-281** (special issue), pp. 243–250.

[13]Akatsuka, C., Honma T., Müller R., Reinsch, S., Tanaka S., & Komatsu T. (2019). Surface crystallization and gas bubble formation during conventional heat treatment in $Na_2MnP_2O_7$ glass. *Journal of Non-Crystalline Solids*. **510**, pp. 36–41.

[14]Müller, R., Zanotto, E.D., & Fokin, V.M. (2000). Surface crystallization of silicate glasses: Nucleation sites and kinetics. *Journal of Non-Crystalline Solids*, **274**(1), pp. 208–231.

[15]Zanotto, E.D. (2013). Glass Crystallization Research - A 36-year retrospective. Part II, Methods of study and glass-ceramics. *International Journal of Applied Glass Science*, **4**(2), pp. 117–124. ■